

RESEARCH ARTICLE

INTEGRATED GEOPHYSICAL, HYDROGEOLOGICAL AND HYDROGEOCHEMICAL ASSESSMENTS OF GROUNDWATER POTENTIALS IN IBIONO IBOM LOCAL GOVERNMENT AREA OF NORTHERN AKWA IBOM STATE, NIGERIA

Ubong D. Ekanem^a, Aniekan E. Edet^b, Nyakno J. George^c, Nsikak E. Bassey^a

^a Department of Geology, Akwa Ibom State University, Ikot Akpaden

^b Department of Geosciences, University of Uyo, Akwa Ibom State

^c Department of Physics, Akwa Ibom State University, Ikot Akpaden.

*Corresponding Author Email: ubongdouglas@gmail.com

This is an open access journal distributed under the Creative Commons Attribution License CC BY 4.0, which permits unrestricted use, distribution, and reproduction in any medium, provided the original work is properly cited

ARTICLE DETAILS

Article History:

Received 10 April 2025

Revised 15 May 2025

Accepted 19 May 2025

Available online 12 June 2025

ABSTRACT

This study presents an integrated geophysical, hydrogeological, and hydrochemical assessment of groundwater potentials in Ibiono Ibom Local Government Area of northern Akwa Ibom State, Nigeria. An electrical resistivity survey was conducted at 39 locations to evaluate aquifer potentials using geoelectrical data. Hydrogeological assessments were carried out to determine aquifer parameters, while hydrogeochemical analyses used Piper trilinear diagrams, Gibbs cross plots and multivariate statistical techniques to assess groundwater quality and facies classification. The 3-layer model is characterized with top layer resistivity from 85.6 Ωm (VES 28) to 1104.9 Ωm (VES 27), layer thickness varied between 0.4 m (VES 1) and 14.3 m (VES 36). Underlying this is a layer of with resistivity values from 812.3 Ωm (VES 34) to 2910.7 Ωm (VES 18) with layer thickness from 9.7 m (VES 1) to 83.2 m (VES 28). Underlying this is a layer with resistivity in the range 102.5 Ωm (VES 18) to 2893 Ωm (VES 34) with unresolved layer thickness. Lithologically, the top layer does not constitute any water bearing medium with underlying layer of unresolved thickness having some conductive zones. The 4-layer geoelectric model has the first layer with thickness and resistivity from 0.8m (VES 10) to 7.3m (VES 26) and 9.2 Ωm (VES 3) to 2312.9 Ωm (VES 17). It is underlain by a layer with resistivity and thickness from 24.8 Ωm (VES 12) to 2943.1 Ωm (VES 32) and thickness 1.4m (VES 11) to 37.4 m (VES 25). The next layer with resistivity and thickness of 23.6 Ωm (VES 9) – 4183.2 Ωm (VES 15) and 8.9m (VES 11) – 136.7.4m (VES 26). The fourth layer with unresolved thickness had resistivity values in the range 4.3 Ωm (VES 10) – 2218.0 Ωm (VES 37). Second, third and fourth layer constitutes the aquifers. The 5- layer geoelectric model has top layer with resistivity and thicknesses from 504.3 Ωm (VES 2) – 2315.2 Ωm (VES 21) and 0.6m (VES 6) – 1.7 m (VES 2). It is underlain by a resistive layer with resistivity and thickness from 64.4 Ωm (VES 2) – 412.6 Ωm (VES 6) and 5.3m (VES 21) – 12.4 m (VES 2). Next is a conductive layer with resistivity and thickness of 281.7 Ωm (VES 2) – 1417 Ωm (VES 21) and 8.4m (VES 21) – 17.8 m (VES 2). This is underlain by a highly conductive layer having thickness from 48.6 m (VES 21) – 57.6 m (VES 6) and resistivity from 57.2 Ωm (VES 6) – 117.6 Ωm (VES 2). The fifth geoelectric layer with unresolved thickness had resistivity in the range 11.1 Ωm (VES 2) – 1205.5 Ωm (VES 21). The fourth and fifth layers constitute the aquifers. Thirty three (33) locations (VES 1,5,6,7,8,9,11,12,13,14,15,16,17,18,19,20,21,22,24,25,26,27,28,31,34,35,36,37 and 38 were identified as promising for groundwater development. Elevation and static water level mean values are 140.13±77.37m and 32.46±17.95m, respectively. The hydraulic conductivity K, averaged 13.28 m/day and the transmissivity T, range from 252.32-1932.24 m²/day (average 413.78 m²/day) for the study area. Groundwater reserves varied between 928.00 x 10⁶ and 64178 x 10⁶ m³ and regional groundwater flow direction is from North to South. Average Fe concentration of 1.67±0.10 mg/L exceeded MAL of 0.37 mg/L. Water is safe for irrigation uses. The hydrochemical facies is classified into 3 groups; the Ca-Mg-HCO₃-Cl, Mg²⁺+Ca²⁺-Cl+HCO₃⁻ and Ca²⁺-Mg²⁺-SO₄²⁻-HCO₃⁻ water types attributed to carbonate and magnesium weathering. Gibb's diagram showed TDS as a function of Na⁺/(Na⁺+Ca²⁺) and Cl⁻/(Cl⁻+HCO₃⁻). Gibbs Cross plots based on chloroalkaline indices CA I and CAII showed forward ion exchange. Factor analysis and multivariate statistical analysis showed loadings suggestive of silicate and carbonate weathering. This study provides critical insights into groundwater suitability for domestic and agricultural uses to support sustainable water resource development given the complex geology of the study area. Preliminary geophysical investigations are recommended before borehole drilling to minimize failure risks.

KEYWORDS

Electrical resistivity, Vertical electrical sounding, Geoelectric, Aquifer, Geophysical, Hydrogeological, Hydrogeochemical, Hydrochemical facies

1. INTRODUCTION

The Sustainable Development Goal (SDG) target 6.1 calls for universal and

Quick Response Code



Access this article online

Website:
www.jcleanwas.com.my

DOI:
10.26480/jcleanwas.01.2025.22.35

equitable access to safe and affordable drinking water. Drinking water from an improved source is available when needed and free from faecal and priority chemical contamination (WHO, 2011). The availability and quality of groundwater resources have been affected by human and natural activities, e.g., infrastructural developments and climate change activities. Groundwater serves as a primary source of drinking water and irrigation in Northern Akwa Ibom State. However, groundwater quality is influenced by a combination of natural geochemical processes and anthropogenic activities, such as agricultural practices, industrial waste disposal, and inadequate sanitation systems. Evaluating groundwater quality through hydrochemical characterization is crucial for sustainable water management (Appelo and Postma, 2005; Todd and Mays, 2005). The availability of groundwater for drinking and agricultural purposes in many regions of the world is a problem due to over-exploitation and contamination of groundwater aquifers (Subba Rao et al., 2012; Bouderbala et al., 2016). Globally, rural communities, particularly in developing nations including Nigeria, have as one of the major problems the lack of adequate potable water supply for domestic use. This is the scenario in several areas, including Ibiono Ibom Local Government Area (LGA) in Akwa Ibom State, because some of the existing water wells which initially produced water have dried up, diminished in yield or produce unsafe water. The funds lost or wasted on such projects would have been properly utilized if suitable drill sites or depths were recommended from detailed hydrogeological or geophysical studies. This is the rationale for this research study on aquifer delineation and hydrochemistry. A greater percentage of rural communities in Nigeria depend on unimproved sources of water for drinking and domestic purposes, and statistics show that just about 75% of boreholes in Nigeria are functional. A quarter of the public water points break down in their first year of completion. About 21% of water points in Nigeria are seasonal, and 47% of boreholes in Nigeria are contaminated with *E. coli*. Two-thirds of boreholes drilled in Nigeria were done without sub-surface investigation (FMWR, 2021). The study area in Ibiono Ibom LGA was selected based on existing hydrogeological challenges, including groundwater depletion, water table variations, and concerns about water quality in northern Akwa Ibom state. Data was obtained from borehole investigations, geophysical surveys, well tests, and laboratory analyses. This integrated methodology enhances the accuracy of groundwater resource assessments by correlating geophysical anomalies with hydrogeological and hydrochemical parameters (Fetter, 2018). The results provide empirical data to guide sustainable groundwater resource management and policy formulation for water supply planning.

The aim of this study is to Integrate geophysical, hydrogeological and hydrogeochemical assessments for sustainable groundwater resources management in Ibiono Ibom LGA of Akwa Ibom state.

The objectives are as follows:

- To delineate the aquifers in the study area using geological and geoelectrical techniques.
- To determine the aquifer parameters based on geoelectrical parameters and hydrogeological data.
- To determine the regional groundwater chemical types, identify the major ion sources and identify the controlling factors influencing the geochemical evolution of the water bodies in the study areas.

To develop a hydrogeoelectrical model and provide recommendations for sustainable groundwater management in the study area.

2. DESCRIPTION OF GEOLOGICAL AND HYDROGEOLOGICAL SETTINGS

Akwa Ibom State lies within latitude 4.9057° N and longitude 7.8537° E and covers an estimated land area of 7,081 km². It is limited to the south by the Atlantic Ocean and, in the north, west and east, by Abia, Imo and Cross Rivers. The study area in Ibiono Ibom LGA of Akwa Ibom State (Figure. 1a) is located within latitude 5.1322° N and longitude 7.9295° E (Udo et al., 2019). The terrain is virtually flat to gently undulating, sloping generally in the direction of the southern part of the state. Elevation is from about 100 to 120 m within the zone. The shale is bluish to dark grey in colour. It is fissile and flat lying. The upper part grades into a mixture of clay and shale and finally into light brownish grey to reddish brown clay. Akwa Ibom State is underlain by sedimentary formations of Late Tertiary and Holocene ages (Short and Stauble, 1967). Deposits of recent alluvium and beach ridge sands occur along the coast and the estuaries of the Imo River and Qua Iboe River, and also along the floodplains of creeks. Inland, a greater part of the state consists of coastal plain sands, now weathered

into lateritic layers, especially in Ini, Ikono, Etinan, Ikot Ekpene, and Itu LGAs. Geologically, Akwa Ibom State is underlain by two main rock types, which are sandstone and mudstone, with some limestone and clay/shale Formations. The geology of Northern Akwa Ibom State is primarily influenced by the Tertiary to Quaternary Formations of the Niger Delta Basin. The dominant lithology includes coastal plain sands, clayey sands, and laterites. The Benin Formation, which is the primary groundwater-bearing unit, consists of highly porous and permeable sandstones interbedded with clay lenses (Short and Stauble, 1967).

Geologically, northern Akwa Ibom is part of the Niger Delta which occupies more than 80% of the study area is made up of Akata Formation (Shales intercalated with sands and siltstone), the Agbada Formation (Sands and Sandstones, intercalated with shales) in the middle and the Benin Formation (coarse-grained sands with minor intercalation of clays) at the top (Short and Stauble, 1967; Murat, 1972). However, Benin Formation, Bende Ameki Group and Imo shales are partly exposed in the study areas. Akwa Ibom State covers a total land area of about 7,081 km², encompassing the Qua Iboe River Basin, the western part of the lower Cross River Basin and the eastern part of the Imo River Basin. The state has an oceanfront which spans a distance of 129 km from Ikot Abasi in the west to Oron in the southeast (Udom, 2004). In the northeastern part of the state, the subsurface geomaterials in the Benin Formation, which include clay and shale, are porous and capable of absorbing water slowly but cannot discharge water in appreciable quantity into a well. The pores of these formations are not interconnected and are only porous but not permeable (Uduak and Ini, 2012). On the basis of geologic succession, four main hydrostratigraphic units have been delineated for the entire state (Esu et al., 1999). These include three aquiferous units designated as upper, middle and lower sand aquifers, in increasing geologic age and depth of burial. The middle aquifer is the most extensive and is separated from the lower sand aquifer by the Imo shale aquitard. These units are thoroughly discussed in chronological order from the youngest using illustrated drilled holes compiled for some existing groundwater wells by (Esu et al., 1999; Edet, 1993).

The hydrology of Akwa Ibom State is defined by a network of rivers, streams, and wetland systems, which significantly influence groundwater recharge. The major rivers in the state include the Cross River, Imo River, and Ikpa River, all of which contribute to surface water flow and aquifer recharge (Ekpo et al., 2017). Hydrogeologically, Akwa Ibom State consists of unconfined to semi-confined aquifers, primarily hosted within the Benin Formation. The aquifer systems are recharged through precipitation, river seepage, and infiltration of surface water. The groundwater table ranges between 5 and 20 meters below the surface, depending on the location and seasonal variations. The transmissivity, T values for the aquifers across the Niger Delta region range from 1.05×10^{-3} m²/s to 11.30×10^{-2} m²/day, while the coefficient of storage or Storativity, S varies between 1.07×10^{-4} and 3.53×10^{-4} , and specific capacity, SC values lie between 19.01 m³/d/m and 139.80 m³/d/m drawdown. These values suggest that the aquifers have very good capacity to transmit groundwater. The specific capacity of a well is its yield per unit drawdown, usually expressed in m³/d/m of drawdown. (Abam and Nwankwoala, 2020). The presence of localized clay beds results in variation in water availability, particularly in areas with lower permeability. The most important aquifers in the Niger Delta are the Deltaic and Benin Formations. Most of the boreholes in the northern parts of the Niger Delta tap unconfined aquifers. In most of these boreholes the geological sequence consists of continuous sandy formations from top to bottom. However, some aquifers occur under confined conditions, resulting in artesian flows. The area is characterized by a humid tropical climate with two seasons, namely, the wet or rainy season and the dry season (Iloje, 2001). The rainy season is from May to October, and the dry season extends from November to April.

3. METHODOLOGY

The study adopts an integrated approach to assessing groundwater potentials using integrating geophysical, geological, hydrogeological and hydrogeochemical techniques. This approach ensures a comprehensive evaluation of the subsurface characteristics, aquifer parameters, and water quality within the study area (Ekanem et al., 2024; Udosen et al., 2024). Other parts of the state had been studied by the use of geoelectrical, geological, hydrogeological and hydrogeochemical methods (Edet 1993; Edet and Ntekim 1996; Esu et al., 1999; Ajayi and Umoh 1998; Edet and Okereke 2001; George et al., 2015a, b,c; Edet and Okereke 2014; Edet 2018). Water quality was analyzed in the laboratory according to the World health organization (WHO) guidelines to assess potability suitability (Ayers and Westcot, 1994). The groundwater samples from 10

boreholes labelled BH1-BH10 were analyzed for major cations, anions and coliforms using standard methods for examining water and wastewater by (APHA, 2017).

3.1 Geoelectric techniques

Geophysical techniques were used to map subsurface structures and identify potential groundwater-bearing formations (Asfahani, 2023). SSR-MP-ATS model of (IGIS) Resistivity meter and its accessories to measure to electrical resistivity of the subsurface. Electrodes were used as the contact points for current to pass into the ground. Cables and clips were utilized to connect resistivity meter to the electrodes. A power source (battery) provided the required power for the survey. Other survey tools such as measuring tapes, compasses were utilized for precise positioning. Garmin channel 12 GPS kit was used to obtain elevations and coordinates for the all locations. The geo-electric survey utilized the Vertical Electrical Sounding (VES) method with the Schlumberger electrode configuration for 39 locations conducted with the maximum current electrode spacing (AB/2) at 300m. With this spacing, the expected depth of penetration varied between 100m and 300m due to clay/shale layers acting as membrane to current penetration. Thirty-nine (39) VES measurements were made in the study area and quantitative interpretations of the geoelectrical data were made by considering the variations in the apparent resistivity for each electrode separation while the point of interest was kept constant. Master curves were used to obtain the resistivity (ρ) and thickness (h) of each geoelectric layer (Zohdy et al., 1974). A data logger was utilized for recording the generated data for future processing and interpretation. WinResist software was utilized for 1D profile modelling and computer-aided interpretation which helped in obtaining better a better resolution of the thicknesses and resistivities of the different geologic layers (Edet and Okereke, 1997).

3.1.1 Estimation of aquifer parameters from geophysical data

To complement areas lacking direct boreholes estimates of aquifer parameters, surface resistivity data was deployed based on the principles of electric and groundwater flow. The examined parameters are expressed as:

$$S = \sum_{i=1}^n \frac{h_i}{\rho_i} \quad (1)$$

S = Longitudinal conductance (in Siemens), h_i (m) = thickness of aquiferous layer and ρ_i (Ωm) = the apparent resistivity of the aquiferous layer

$$Tr = \sum_{i=1}^n \rho_i h_i \quad (2)$$

Tr = Transverse resistance which is a product of the apparent resistivity and thickness of the aquiferous layer

$$T = Kh \quad (m^2/day) \quad (3)$$

$K = Th^{-1}$, h = aquifer thickness (m).

where T, K, are aquifer transmissivity and hydraulic conductivity. From results of surface resistivity measurements, Dar Zarrouk parameters were computed according to the study in Equations 1, 2 and 3 (Maillet, 1947), (Bhattacharya and Patra, 1968; Asfahani, 2023).

A relationship between aquifer transmissivity, transverse resistance and longitudinal conductance has been established (Niwas and Singhal, 1981). Therefore, equations 1, 2 and 3 in Dar Zarrouk parameters can be combined to give equations 4, 5 and 6 (Massoud et al., 2022):

$$T = (K\sigma R) \quad (4)$$

Where R = Transverse resistance

$$T = \left(\frac{K}{\sigma}\right) C \quad (5)$$

Where C = longitudinal conductance

and

$$K = \frac{T}{h} \quad (6)$$

Where σ is water electrical conductivity (Siemens/m or $\mu S/cm$). In areas of similar geological and water quality characteristics, the product $K\sigma$ will remain fairly constant (Niwas and Singhal, 1981; Mbonu et al., 1991; Onuoha and Mbazi, 1988; Tizro et al., 2010). Therefore, if K values are known from the pumping test and σ from the resistivity measurements, it is possible to calculate transmissivity and its variations over the entire aquifer.

3.1.2 Groundwater reserve estimation

The total amount of groundwater reserve (GR) for the hydrogeological zones was determined as follows (Edet and Okereke, 2014):

$$GR = Atn(m^3) \quad (7)$$

Where A is the area m^2 , t is the saturated thickness of the aquifer obtained from geoelectric sounding and water level measurements in m and n porosity in %.

3.2 Geologic and hydrogeologic techniques

A system of geological and hydrogeological investigation was conducted on 7 boreholes in 7 LGA's of northern Akwa Ibom state, including the study area for the purpose of comparison due to the heterogeneity of geological formations therein. Lithological logs were collected to complement the geophysical studies, decipher the aquifer materials and static water levels. Aquifer parameters were determined using geoelectrical results and standard hydrogeological data.

3.3 Hydrochemical techniques

Field measurements taken during the study include; geographic coordinates and elevation using the GPS Garmin type 76 kits. The groundwater samples from 10 boreholes labelled BH1-BH10 were analysed for major cations and anions using standard methods for examination of water and wastewaters by (APHA, 2017). To study the physical, chemical and bacteriological water qualities of the groundwater within the area, to determine the dominant cations and anions and their influence on the area, compare the results of the study with international specification in order to determine their suitability for domestic, irrigation and industrial uses (WHO, 2011).

3.3.1 Hydrochemical facies

Hydrochemical plots included Piper Trilinear diagrams and Gibbs Cross Plots are used to simulate the hydrochemical processes operating in the groundwater system and shows the relative concentrations of the different ions from the individual samples based on average values for each location within the area of study. It also permits the cations and anion compositions of characterizing the various groundwater types within the area. The Piper's trilinear diagram is one of the most common methods for presenting hydrochemical facies (Back and Hanshaw, 1965; Piper, 1944).

3.3.2 Multivariate statistics

Pearson moment correlation analysis and factor analysis were employed to understand the degree of association of the physico-chemical parameters. Correlation describes the size and direction of the linear relationship between two contiguous variables and ranges in value from -1 to +1. When one variable increases as the 2nd increases, correlation is positive while if the variables vary in opposite direction correlation is negative (Kalaivani and Krishnaveni, 2015). Factor analysis explains the correlations between sample observations in the field. The technique reduces a large number of variables into smaller dataset without the loss of information (Williams et al., 2010).

4. RESULTS AND DISCUSSIONS

Thirty-nine (39) VES measurements and 10 water samplings made in the study area are displayed on the geological map in Figure. 1b. Table 1 gives a summary of the VES numbers, layer resistivity values, number of layers, thicknesses and depth to aquifer in the study area. Table 1 give the following information about the VES stations: the field name of the station; the geographical location of each station; the number of geological layers present at the subsurface of each station; the resistivity of these layers; the thickness of each layer, the total depth of each layer from the surface and the lithology. The VES locations in the study area generally fit 3 layers of A ($\rho_1 > \rho_2 > \rho_3$), K ($\rho_1 < \rho_2 > \rho_3$) and H ($\rho_1 > \rho_2 < \rho_3$) and 4 layers of HK ($\rho_1 > \rho_2 < \rho_3 > \rho_4$) and QH ($\rho_1 > \rho_2 > \rho_3 < \rho_4$) types (Table 1).

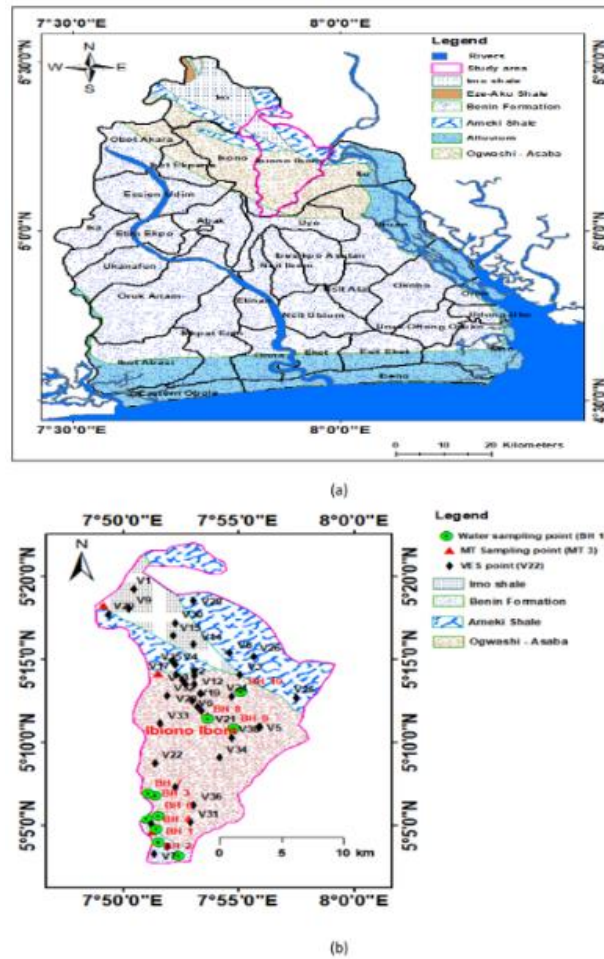


Figure 1: (a); Geological map of Akwa Ibom State showing the study area. (b); Geological map of study area showing the 39 VES points and 10 water sampling points

4.1 Hydrogeoelectrical layers

The 3-layer model is characterized by VES locations 1, 18, 27, 28, 31, 34 and 36 in the study area (Table 1). The top layer with resistivity from 85.6 Ωm (VES 28) to 1104.9 Ωm (VES 27). The layer thickness of this layer varied between 0.4 m (VES 1) and 14.3 m (VES 36). Underlying this is a layer of with resistivity values from 812.3 Ωm (VES 34) to 2910.7 Ωm (VES 18) with layer thickness from 9.7 m (VES 1) to 83.2 m (VES 28). Underlying this is a layer with resistivity in the range 102.5 Ωm (VES 18) to 2893 Ωm (VES 34) with unresolved layer thickness. Lithologically, the top layer represents unsaturated overburden composed of fine-medium grained, clayey, silty, lateritic sand and does not constitute any water bearing medium. Underlying this is a layer of conglomerates. Underlying this is a layer of with unresolved thickness which represents silty, clayey, gravelly, fine-coarse sand and gravels with some conductive zones. The layer is composed of clayey, silty fine-coarse sand.

The 4-layer geoelectric models were encountered at VES locations 3, 5, 7, 8, 9, 10, 11, 12, 13, 14, 15, 16, 17, 19, 20, 22, 23, 24, 25, 26, 29, 30, 32, 33, 35, 37, 38 and 39 in the study area (Table 1). The first layer with thickness and resistivity from 0.8m (VES 10) to 7.3m (VES 26) and 9.2 Ωm (VES 3) to 2312.9 Ωm (VES 17). The top layer is underlain by a layer with resistivity and thickness from 24.8 Ωm (VES 12) to 2943.1 Ωm (VES 32) and thickness 1.4m (VES 11) to 37.4 m (VES 25). The second layer with resistivity and thickness of 23.6 Ωm (VES 9) – 4183.2 Ωm (VES 15) and 8.9m (VES 11) – 136.7.4m (VES 26). The fourth layer with unresolved thickness had resistivity values in the range 4.3 Ωm (VES 10) – 2218.0 Ωm (VES 37) in the study area. Lithologically, the first layer reveals top soil composed of

dry loose silty, sandy, clayey, gravelly materials of no hydrogeologic significance. The top layer is underlain by slightly conductive layer which constitutes the first aquifer. Borehole data show that the layer is composed of clayey, silty, gravelly saturated sand. The second layer is followed by a conductive layer composed of saturated clayey, silty, sand and constitutes the second aquifer in the study area. The fourth layer with unresolved thickness constitutes the third aquifer in the area, which is not currently exploited. The layer is composed of gravelly, silty, clayey sand.

The 5-layer geoelectric models were encountered at VES locations 2, 6, and 21, (Table 1). The data revealed a top layer with resistivity and thicknesses from 504.3 Ωm (VES 2) – 2315.2 Ωm (VES 21) and 0.6m (VES 6) – 1.7 m (VES 2). The top layer is underlain by a resistive layer with resistivity and thickness from 64.4 Ωm (VES 2) – 412.6 Ωm (VES 6) and 5.3m (VES 21) – 12.4 m (VES 2). The second geoelectric layer is followed by a conductive layer with resistivity and thickness of 281.7 Ωm (VES 2) – 1417 Ωm (VES 21) and 8.4m (VES 21) – 17.8 m (VES 2). The third layer is underlain by a highly conductive layer having thickness from 48.6 m (VES 21) – 57.6 m (VES 6) and resistivity from 57.2 Ωm (VES 6) – 117.6 Ωm (VES 2). The fifth geoelectric layer with unresolved thickness had resistivity in the range 11.1 Ωm (VES 2) – 1205.5 Ωm (VES 21). The lithological data revealed a top layer composed of dry loose reddish yellowish unconsolidated silty, sandy, gravelly material. The first and second geoelectric layers do not hold any prospect for groundwater. The second geoelectric layer is followed by a conductive layer composed of coarse/gravelly sand. The third layer is underlain by a highly conductive layer. The fifth geoelectric layer has unresolved thickness with the fourth and fifth layers constituting the aquifers.

Table 1: VES summary with number of layers and lithology of the study area

VES No.	No. of Layers	Curve Type	Resistivity (Ωm)	Thickness (m)	Depth (m)	Lithology
1	3	K	176.5	0.4	0.4	Top soil
			2855.3	9.7	10.1	Conglomerate
			1635.4			Medium to coarse grain sand
7	4	KQ	262.8	4.1	4.1	Lateritic soil

Table 1 (cont): VES summary with number of layers and lithology of the study area

			755.5	30.0	34.0	Small to medium grained sand
			241.1	75.8	109.6	Fine grained sand with minor clay intercalations (saturated at 63m)
			89.1			Shale formation
10	4	KQ	193.4	0.8	0.8	Top soil
			2573.6	14.2	15.	Conglomerate
			179.6	71.9	86.9	Fine grained sand with minor clay intercalations (saturated at 69m)
			4.3			Shale formation
3	4	KH	9.2	1.2	1.2	Top soil
			330	5.5	6.7	Fine grain sand
			73	127.4	134.1	Shale formation
			71.5			Shale formation
5	4	KH	347.1	1.3	1.3	Top soil
			1388.4	22.6	23.9	Medium grained sand
			231.9	70.9	94.8	Fine grained sands
			811.3			Fine to medium grained sand
8	4	KH	337.8	1.3	1.3	Top soil
			1449.1	19.9	21.2	Conglomerate
			283	95.2	116.5	Fine grained sand with minor clay intercalations (saturated at 59m)
			826.5			Fine to medium grain sand
9	4	KH	79.8	1.0	1.0	Top Soil
			2119.2	2.6	3.6	Sand stone
			23.6	16.9	20.4	Clay
			83.2			Aquiferious Zone
12	4	HA	226.1	3.5	3.5	Lateritic soil
			24.8	4.7	8.2	Shale formation
			3054.5	109.9	118.2	Coarse grained sands
			506.2			Fine to medium grained sand
20	4	HA	615.5	1.9	1.9	Top soil
			53.7	13.3	15.2	Shale formation
			4953	94.4	109.6	Coarse grained sands
			583.2			Fine to medium grained sand
19	4	HQ	733.5	2.7	2.7	Top soil
			60.5	24.4	27.2	Shale formation
			176	90.9	118.0	Fine grained sands with clay intercalation
			468.7			Fine to medium grained sand
2	5	HKQ	504.3	1.7	1.7	Top Soil
			64.4	12.4	14.1	Clay Sand
			281.7	17.8	31.9	Lateritic Clay
			117.6	52.6	84.3	Clayey Material
			11.1			Clayey Material
6	5	HKQ	2126	0.6	0.6	Top soil
			412.6	6.6	7.2	Lateritic soil
			1338	9.6	16.8	Medium to coarse grain sands with clay intercalation (saturated at 85m)
			57.2	57.6	74.4	Fine grain sand
			1002.2			Medium to coarse grain sand
11	4	HK	2075.8	1.5	1.5	Top soil
			624.7	1.4	2.9	Mottles mud
			2980.0	8.9	11.6	Conglomerate
			164.3			Shale formation
13	4	HK	1806.4	2.4	2.4	Top soil
			1407.1	2.5	4.9	Lateritic soil

Table 1 (cont): VES summary with number of layers and lithology of the study area

			2910.6	16.8	21.7	Conglomerate
			383.7			Fine grain sand
16	4	KH	1922.5	1.4	1.4	Top soil
			2676.5	15.7	17.1	Conglomerate
			654.3	109.8	126.9	Fine grain sand
			894.9			Fine to medium grain sand with clay intercalation
17	4	KH	2312.9	7.0	7.0	Lateritic soil
			2906.8	18.8	25.8	Conglomerate
			238.7	68.3	94.1	Fine grain sand with clay intercalation
			564.0			Fine to medium grain sand
21	5	HKQ	2126	0.6	0.6	Top soil
			412.6	6.6	7.2	Laterite
			1338	9.6	16.8	Coarse grained sands
			57.2	57.6	74.4	Shale formation
			1002.2			Medium to coarse grain sand
14	4	KQ	1569.1	1.3	1.3	Top soil
			2685.3	9.7	11.1	Conglomerate
			461.5	39.2	50.3	Fine grain sand
			126.8			Fine grain sand with clay intercalation
15	4	KQ	1467.1	1.4	1.4	Weathered mudstone
			2564.2	9.3	14.8	Consolidated conglomerate
			4183.2	19.0	108.8	Silt stone
			472.7			Medium grain sand (saturated)
18	3	K	850.1	4.5	4.5	Lateritic soil
			2910.7	12.8	17.3	Conglomerate
			102.5			Fine grain sand with clay intercalation
22	4	HK	1224.1	3.9	3.9	Lateritic soil
			740.1	5.7	9.5	Medium grain sand
			2908.1	111.0	120.6	Conglomerate
			758.1			Fine to medium grain sand
23	4	AK	385.6	4.1	4.1	Lateritic soil
			1033.1	10.9	15.1	Medium to coarse grain sand
			2155.3	92.2	107.3	Conglomerate
			839.4			Medium grain sand
24	4	AK	464.6	2.0	2.0	Top soil
			2281.8	8.8	10.8	Coarse grain sand with spaced pebbles
			2901.7	48.3	59.1	Conglomerate
			629.5			Medium grain sand
25	4	AK	517.7	1.0	1.0	Top soil
			1373.1	37.4	38.5	Medium to coarse grain sand
			2770.0	94.6	133.1	Conglomerate
			1172.5			Medium to coarse grain sand
26	4	HK	953.1	7.3	7.3	Lateritic soil
			605.3	20.7	28.1	Fine grain sand
			2934.6	136.7	164.8	Conglomerate
			1923.0			Coarse grain sand
27	3	K	1104.9	6.0	6.0	Lateritic soil
			2725.2	15.4	21.5	Conglomerate
			973.7			Medium grain sand
28	3	K	85.6	5.1	5.1	Top soil
			2612.4	83.2	88.3	Medium grain sand
			674.5			Conglomerate
29	4	KH	463.4	1.2	1.2	Top soil
			1252.6	10.0	11.2	Medium to coarse grain sand

Table 1 (cont): VES summary with number of layers and lithology of the study area

			1025.5	121.7	132.9	Medium to coarse grain sand with clay intercalation
			1556.7			Coarse grain sand
30	4	HK	301.1	0.9	0.9	Top soil
			81.2	20.4	21.2	Medium to coarse grain sand
			627.1	72.4	93.6	Medium to coarse grain sand with clay intercalation
			126			Coarse grain sand
31	3	K	788.0	1.8	1.8	Top soil
			2839.5	36.9	38.7	Conglomerate
			788.1			Fine to medium grained sand
32	4	KQ	1223.1	1.1	1.1	Top soil
			2943.1	2.0	3.1	Conglomerate
			734.3	89.5	92.6	Fine to medium grained sand
			400.5			Fine grain sand
33	4	KQ	396.2	1.0	1.0	Top soil
			985.4	2.1	3.1	Medium grain sand
			200.9	23.7	26.8	Fine grain sand
			128.8			Clay sand
34	3	A	475.9	1.8	1.8	Top soil
			812.3	10.8	12.6	Medium grain sand
			2893.0			Conglomerate
35	4	HK	527.6	5.7	5.7	Lateritic soil
			143.9	5.1	10.8	Clay sand
			2896.8	21.8	32.6	Conglomerate
			13.7			Shale formation
36	3	K	618.5	14.3	14.3	Lateritic soil
			1540.9	73.3	87.6	Coarse grain sand
			647.0			Fine grain sand
37	4	AK	1005.1	2.7	2.7	Lateritic soil
			1489.4	17.5	20.2	Coarse grain sand
			2896.2	83.6	103.8	Conglomerate
			2218.0			Coarse grain with spaced pebbles
38	4	HK	537.7	2.3	2.3	Top soil
			244.0	4.5	6.9	Mottle mud
			2906.3	89.5	96.4	Conglomerate
			1864.9			Coarse grain sand
39	4	HK	529.3	1.6	1.6	Top soil
			314.9	3.0	4.6	Mottle mud
			2927.4	90.4	95.0	Conglomerate
			1061.7			Coarse grain sand

4.1.1 Interpretation of representative geoelectric curves

Data interpretation showed the models for VES 3, a thin fine-grained sand unit 1.2m thickness of extending to 6.7 m depth, followed by a substantial shale formation reaching 134.1 m. The presence of continuous shale Formation at greater depths suggests low groundwater potential, making this location unsuitable for borehole drilling. The curve is KH type (Figure. 2a).

For VES 5, the location exhibits a thin topsoil layer, 1.3 m thick, followed by medium-grained sand extending to 23.9 m depth. A thick fine-grained sand unit reaching 94.8 m suggests a potential aquifer, with underlying fine to medium-grained sand providing additional groundwater storage

potential. The combination of sand units suggests moderate-to-high groundwater yield prospects. The curve is KH type (Figure. 2b).

For VES 7, the location exhibits a thick topsoil layer, 4.1 m thick, followed by medium-grained sand extending to 34.0 m depth. A fine grained sand with minor clay intercalations (saturated at 63m) reaching 109.8 m suggests a potential aquifer, with underlying Shale Formation forming a semi-confined aquifer. The combination of suggests moderate-to-high groundwater yield prospects. The curve is KQ type (Figure. 2c).

For VES 8, the location exhibits a thick topsoil layer, 4.1 m thick), followed by conglomerate extending to 21.2 m depth. A Fine grained sand with minor clay intercalations (saturated at 59m) reaching 116.5 m suggests a

potential aquifer, with underlying Fine to medium grain sand. The combination of suggests moderate-to-high groundwater yield prospects.

The curve is KH type (Figure. 2d).

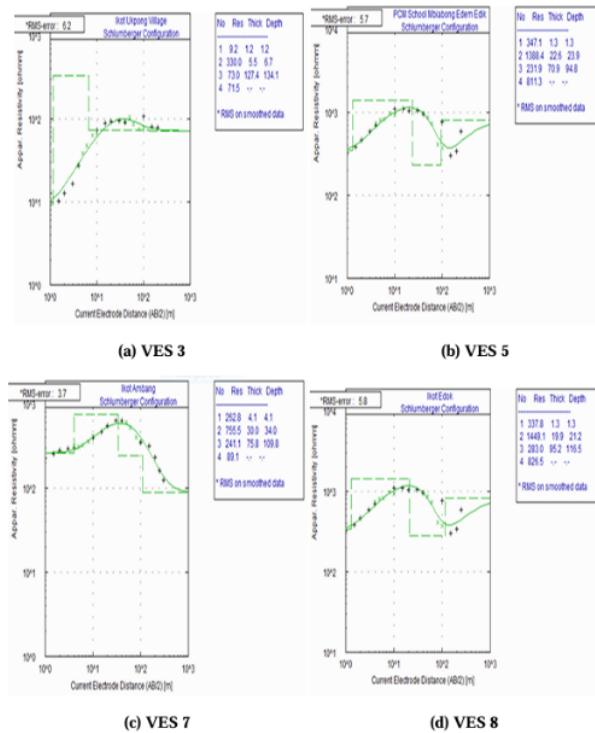


Figure 2: Profile illustrating four selected interpreted 1D models of (a) VES 3, (b) VES 5, (c) VES 7, (d) VES 8 of the VES data in the study area

4.1.2 Hydrogeoelectrical profiles

A north-south cross section of the study area through VES locations 11, 15, 8, 7 and 19 revealed 4 geoelectric layers (Figure. 3a). The top layer (A) with resistivity from 262.8 Ωm (VES 7) – 2075.8 Ωm (VES 11) correspond to top soil. The thickness of this layer is generally < 5m and has no hydrogeologic significance. Underlying the top layer is resistive layer at VES 15 and conductive layers at VES 8 and VES 7. This layer corresponds B₁ (VES 15, VES 7) and B₂ (VES 15) and D (VES 8). At VES 19, this layer B₃ with resistivity of 60.5 Ωm correspond to clayey/shaly material. Underlying the second layer is the third layer with resistivity from 241.1 Ωm (VES 7) – 4183.2 Ωm (VES 15). This layer corresponds to B₂ at VES 11 and VES 15 and B₁ at VES 8, VES 7 and VES 19. This layer constitutes the first aquifer at VES 8, VES 7 and VES 19, all in the southern parts of the study area. The third layer is underlain by a conductive layer at VES 11 (164.3 Ωm) and VES 7 (89.1 Ωm) corresponding to B₃. The highly resistive layer at VES 15 (4183.2 Ωm) correspond to B₂ and probably the second aquifer. This layer is also characterized by resistivity value of 826.5 Ωm (VES 8) and 468.7 Ωm (VES 19). This corresponds to B₁ and constituting

another aquifer.

4.1.3 Hydrostratigraphy

Lithologically, this group consists of alternating clays, lateritic clays, sandy clays, fine to coarse sands, clayey sands, clayey gravels, lignite, and shales (Mbiatok, IB1, Ono IB2, Etimbok IB3 and Oko-Ita IB4). The clay horizons and lenses disturb the vertical and lateral continuity of aquifers and locally produce multiaquifer systems (Figure. 3b). The identification of hydrostratigraphic units in this group (5) is very complicated due to the distribution of different types of sentiments. In the delimitation of hydrostratigraphic units, lithologic, geophysical and hydraulic data are used. The thickness of the saturated zone varies from 6m at Oko-Ita (IB4) to 200m at Mbiatok (IB1). Depth to the top of the saturated zone varies between 4m at Etimbok (IB3) to about 200m at Mbitok (IB1). The saturated thickness depends on mainly the seasonal fluctuations and rate of withdrawal. The static water level, SWL varies between 34.75m at Oko-Ita (IB4) to 48m at Ono (IB2) with a mean of 38.11±6.59 m. The elevation mean value of elevation is about 90.50±6.83 m.

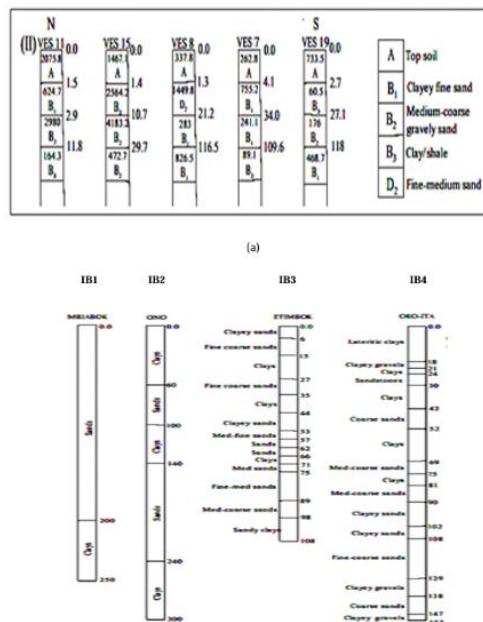


Figure 3: (a) Hydrogeoelectrical section of study area. (b); Hydrostratigraphic Section through parts of the study area

4.2 Aquifer parameters

Pumping and static water level tests were conducted in 7 LGA’s, including the study area, in northern Akwa Ibom state, (Figure. 4a). All the boreholes are located in the northern part of the state noted for its complex geology regarding groundwater availability. The justification for the comparison is based on the heterogeneity of the formations located therein and used to determine those with favourable aquifer parameters. Relevant data of aquifer parameters from the 7 sampled wells defining the dynamics of the well hydraulics were used computed and used for a comparative analysis..

Table 2 presents the values of aquifer transverse resistance (R) and aquifer longitudinal conductance (C) computed from equations 1 and 2 and T from equations 3, and 5. The parameter $K\sigma$ which is constant for the aquifer was estimated for well locations well-6. This was combined with transverse resistance values from other locations without pumping test data to determine the hydraulic conductivity and transmissivity of the aquifer. The hydraulic conductivity, K values averaged 13.28 m/day and the transmissivity values were in the range of 252.32-1932.24 m²/day (average 413.78 m²/day) for the study area.

Table 2: Estimated aquifer parameters obtained from VES data for the study area.

No	Parameter/location	Ibiono Ibom						
	VES No	7	7	8	8	15	15	19
	Aquifer No	1	2	1	2	1	2	1
1	average field hydraulic conductivity, K (m/day)	13.28	13.28	13.28	13.28	13.28	13.28	13.28
2	transmissivity (m ² /day)	413.78	413.78	413.78	413.78	413.78	413.78	413.78
3	aquifer resistivity, ρ_a (Ω m)	755.2	241.0	1449.1	283.0	8183.2	5472.7	4953.0
4	aquifer thickness, t (m)	30.00	75.80	19.90	95.20	19.00	145.50	94.40
5	aquifer longitudinal conductance, C (Ω ⁻¹)	0.04	0.31	0.01	0.34	0.00	0.03	0.02
6	aquifer transverse resistance, R (Ω m ²)	22656	18267.8	28837.09	26941.6	155480.8	796277.9	467563.2
7	$\sigma = 1/\rho$	0.001	0.004	0.001	0.004	0.000	0.000	0.000
8	K/ σ value	10029.06	3200.48	19244.05	3758.24	108672.9	72677.46	65775.84
9	$K\sigma$	0.018	0.055	0.009	0.047	0.002	0.002	0.003
10	transmissivity of aquifer, T (m ² /day)	398.4	1006.624	264.272	1264.256	252.32	1932.24	1253.632
11	hydraulic conductivity of aquifer K (m/day)	13.28	13.28	13.28	13.28	13.28	13.28	13.28

Remarks: σ electrical conductivity (Siemens/m)

4.2.1 Static water level and groundwater flow direction

The elevation of water level ranged between 36.40 m amsl to 178.40 m with mean 107.40±100.41 m. Average recorded SWL value was 42.50±6.36 m. Static water level (SWL) data from well-12 and well-13 in the study area in Figure. 4a shows that the SWL varied between 34.75 m and 35.20 m with mean of 34.98±0.32 m. Absolute water level (AWL)

varied between 50.80 m and 60.25 m with a mean of 55.53±6.68 m for the study area. Elevation of water level ranged from 74.40 m to 225.40 m with a mean of 140.13±77.37 m, SWL values ranged from 12.40 m to 47.00 m with a mean of 32.46±17.95 m, AWL value ranged from 36.60 m to 178.40 m and a mean of 107.73±70.90 m for the study area. The regional groundwater flow direction obtained from 4 wells as shown in Figure. 4b is from North to South in the study area.

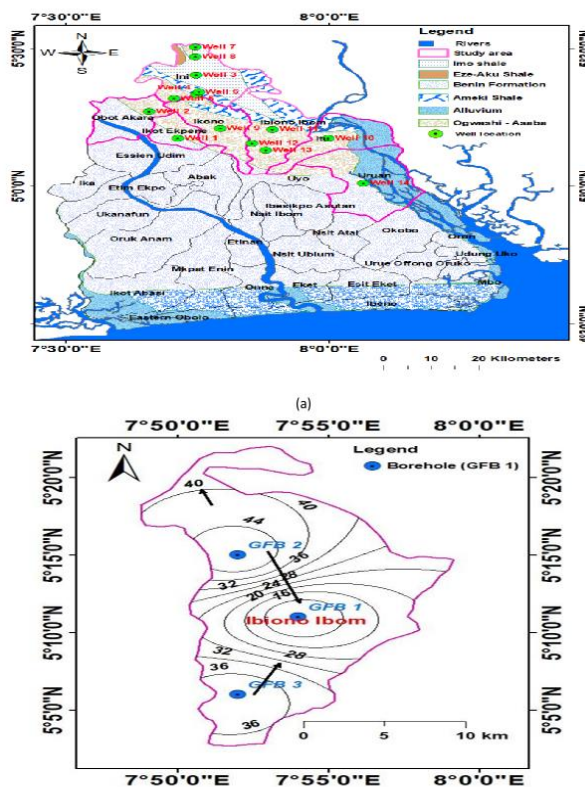


Figure 4: (a); Geological map of Akwa Ibom State showing 7 LGA’s sites for pumping and static water level tests. (b); Contour map showing the groundwater flow direction in the study area

4.2.2 Groundwater reserve estimation

With an estimated area of 1,020,408,163.27 m² for the study area and an average porosity of 35% the groundwater reserves varied between 928.00 x 10⁶ and 64178 x 10⁶ m³ for the study area (Freeze and Cherry, 2010). This suggest enormous amount of groundwater that can be sustainably developed, especially for the rural residents.

4.2.3 Groundwater quality for drinking

The univariate statistical summary values of the physicochemical and microbiological parameters and heavy metals of groundwater resources in the study area are compared with those in Table 3 (WHO, 2011). The standard deviation (SD) exhibited low variations (< 5) in all the parameters indicating that the water might have been not been affected by different hydrochemical processes. The physicochemical parameters and heavy metals in the water are below the maximum admissible limits (MAL) in Table 3 (WHO, 2011).

The mean values of groundwater temperature for the study area were found to be 28.16±0.55°C and fall within the ambient temperature levels of 22 °C to 29°C (Stumm and Morgan, 2012). The pH is a measure of the acidity or alkalinity of water. The mean pH values of groundwater were found to be 6.41±0.26 for the study area. Common range of pH in natural water falls within 6 to 8 (Thakre et al., 2010). Majority of the water samples have pH values within this range. On the basis of mean values, the water is classed as slightly acidic (pH < 6). Electrical conductivity (EC) is also a measure of total dissolved solids (TDS), which measure the amount of dissolved salts in water and general quality of water. Recorded mean EC values were 213.99±1.83 µS/cm. The mean values of TDS recorded were 117.83±3.44 mg/L. EC and TDS values were below the maximum admissible limit (MAL) of 1500 µS/cm and 1000 mg/L.

The mean recorded values of total hardness (TH) 105.36±2.18 mg/L. On the basis of TH (< 500 mg/L) all the water samples are soft and suitable

for drinking and domestic use.

Sodium and potassium occur naturally in water due to seawater intrusion and silicate weathering (Edet, 2018; Edet 2021, Edet and Okereke 2001, 2022). The mean concentration of Na⁺ was 7.06±0.46 mg/L. The mean concentration of K⁺ was 6.41±0.29 mg/L. The concentrations of sodium and potassium were found to be within the MAL of 200 mg/L and 12 mg/L.

Average concentration of Ca²⁺ was 27.34±1.12 mg/L. The mean concentration of Mg²⁺ in was 11.24±0.72 mg/L. The concentrations of calcium and magnesium were found to be within the MAL of 75 mg/L and 150 mg/L.

Chloride occurs naturally in water of all types. However, elevated concentration could be due to runoff of inorganic fertilizer, sewage discharge, sea water intrusion and halite dissolution (Edet and Okereke, 2002; Lkr et al., 2020; Edet and Okereke 2001, Edet 2021). The average concentrations of Cl⁻ was 22.50 ±1.14 mg/L were below the MAL of 250 mg/L. The average concentrations of bicarbonate were 34.50±2.92 mg/L. The concentration of bicarbonate was found to be within the MAL of 600 mg/L. Sulphate occurs naturally in water due to weathering of country rock, leachate, air deposition and industrial waste water (Lkr et al., 2020). The mean concentration of SO₄²⁻ recorded in the different water types was 15.75±1.22 mg/L. All the observed values were within MAL value of 250 mg/L. Nitrate is found in water as a result of fertilizer runoff and waste disposal. Moreover, ingestion of water with high nitrate may results in high risk of methemoglobinemia (Mukherjee and Singh 2021; 2022). The average concentration of nitrate was 4.08±0.31 mg/L. Concentrations of were below the MAL of 45 mg/L.

The concentration of coliform in groundwater 0.00±0.00 cfu/ml, which are within the WHO MAL of 0.00 cfu/ml. In the study area, Fe concentration averaged 1.67±0.10 mg/L. All the groundwater samples had Fe concentration higher than MAL of 0.37 mg/L, which attributable to natural geogenic sources. Mn concentration averaged 0.14±0.03 mg/L.

Table 3: Statistical summary of the physicochemical parameters and heavy metals for groundwater in study area

Parameter	BH 1	BH 2	BH 3	BH 4	BH 5	BH 6	BH 7	BH 8	BH 9	BH 10	Min	Max	Mean	SD	WHO (2011)
Temp (°C)	28.9	28.5	27.9	28.3	27.2	28.2	27.4	28.1	28.8	28.3	27.20	28.90	28.16	0.55	-
pH	6.3	6.2	6.7	6.2	6.5	6.3	6.1	6.3	6.6	6.9	6.10	6.90	6.41	0.26	6.5-8.5
EC (µS/cm)	213.4	211.4	215.5	217.4	215.1	213.5	214.2	212.5	215.3	211.6	211.40	217.40	213.99	1.89	1500
TDS (mg/L)	118.71	117.32	113.63	115.35	116.42	119.53	124.3	121.83	117.63	113.53	113.53	124.32	117.83	3.44	1000
Total Hardness (mg/L)	107.85	108.1	105.5	102.4	104.4	105.3	108.5	104.3	102.6	104.6	102.40	108.50	105.36	2.18	500
Na ⁺ (mg/L)	6.3	7.1	6.8	7.5	6.9	7.1	7.8	7.4	6.5	7.2	6.30	7.80	7.06	0.46	500
K ⁺ (mg/L)	6.42	6.51	6.15	6.35	6.24	6.12	6.36	6.32	7.13	6.53	6.12	7.13	6.41	0.29	200
Ca ²⁺ (mg/L)	26.2	28.3	27.3	25.7	26.9	28.4	27.3	26.4	27.5	29.4	25.70	29.40	27.34	1.12	12
Mg ²⁺ (mg/L)	10.38	11.54	10.94	10.51	12.35	11.36	10.53	11.62	12.32	10.84	10.38	12.35	11.24	0.72	75
Cl ⁻ (mg/L)	20.5	23.4	21.4	25.2	22.4	21.3	23.3	21.4	23.6	22.5	20.50	25.20	22.50	1.14	150
HCO ₃ ⁻ (mg/L)	35	39	31	33	37	31	33	38	32	36	31.00	39.00	34.50	2.92	250
SO ₄ ²⁻ (mg/L)	14.25	16.32	15.84	18.43	15.73	14.57	15.54	14.74	15.32	16.74	14.25	18.43	15.75	1.22	600
NO ₃ ⁻ (mg/L)	3.62	4.52	3.94	4.14	4.37	3.89	4.53	4.15	3.94	3.74	3.62	4.53	4.08	0.31	250
Fe (mg/L)	1.6	1.73	1.58	1.69	1.6	1.85	1.74	1.68	1.52	1.74	1.52	1.85	1.67	0.10	50
Mn (mg/L)	0.15	0.12	0.11	0.16	0.13	0.12	0.14	0.19	0.11	0.18	0.11	0.19	0.14	0.03	0.3
Coliform (cfu/ml)	0	0	0	0	0	0	0	0	0	0	0.00	0.00	0.00	0.00	0.2

4.2.4 Groundwater quality for irrigation

4.2.4.1 Electrical conductivity

Electrical conductivity (EC) is often used to assess the salinity of water (Massoud et al., 2022). The EC values varied as follows: 211.40 $\mu\text{S}/\text{cm}$ and 217.40 $\mu\text{S}/\text{cm}$. The EC results revealed that 100% of the groundwater samples for both LGAs have EC values < 250 $\mu\text{S}/\text{cm}$ which reflects no restriction for irrigation.

4.2.4.2 Sodium adsorption ratio

Sodium adsorption ratio (SAR) compares the percentage of sodium ions in water to calcium and magnesium ions. SAR is inversely proportional to the rate of water percolation in soil (Massoud et al., 2022).

From the equation;

$$SAR = \frac{Na}{\sqrt{\frac{Ca + Mg}{2}}} \quad (8)$$

The average values of SAR were 0.29 ± 0.02 meq/L indicating that these samples are appropriate for irrigation (SAR < 10).

4.2.4.3 Percent Sodium

From the equation; $\text{Na}\% =$

$$\frac{Na + K}{Ca + Mg + Na + K} \quad (9)$$

The average values of %Na were 17.00 ± 0.81 meq/L for the study area indicating that these samples are appropriate for irrigation.

4.2.4.4 Residual sodium carbonate

Residual sodium carbonate (RSC) was used to assess the dangerous impact of HCO_3^- and CO_3^{2-} on irrigation water quality and measure the effects of HCO_3^- and CO_3^{2-} on soil and crop development (Massoud et al., 2022; Aghazadeh and Mogaddam 2010). From the equation;

$$RSC = (Co_2 + HCo_3) - (Ca + Mg) \quad (10)$$

The average RSC values were -1.64 meq/L to -1.36 meq/L with an average of -1.92 ± 0.09 meq/L for the study area and this indicates safe irrigation water.

4.2.4.5 Magnesium hazard

From the equation;

$$MH = \frac{(Mg^{2+})}{(Ca^{2+} + Mg^{2+})} \quad (11)$$

The average magnesium hazard (MH) values were 0.29 ± 0.02 meq/L for the study area indicating that these groundwater samples are appropriate for irrigation.

4.2.4.6 Permeability index

From the equation;

$$PI = 100 \times \left(Na^+ + \sqrt{HCO_3^-} \right) / \left(Ca^{2+} + Mg^{2+} + Na^+ \right) \quad (12)$$

The average Permeability index (PI) values were 35.27 ± 1.70 meq/L for the study area indicating that these groundwater samples are appropriate for irrigation.

4.3 Hydrochemical facies

Plotting of the analytical results on a Piper diagram (Figure. 5i) revealed that the hydrochemical facies of the different water types are classified into three groups. The first group is the Calcium-magnesium-Bicarbonate-Chloride (Ca-Mg- HCO_3 -Cl) water type. 80% of the samples in the study area fall within the first group (Massoud et al., 2022). These facies are attributed to carbonate weathering and Base Exchange. The second group is Magnesium-Calcium-Chloride-Bicarbonate ($\text{Mg}^{2+} + \text{Ca}^{2+}$ -Cl- HCO_3^-). The group consists of 20% of groundwater from the study area. This facies signifies magnesium weathering. The third group is Calcium-Magnesium- Sulphate-Bicarbonate (Ca^{2+} - Mg^{2+} - SO_4^{2-} - HCO_3^-). This group consists of all the water samples from the study area. This group is related to silicate weathering, Base Exchange, ion exchange and human induced activities (Mukherjee and Singh, 2022).

4.3.1 Sources of ions

Using the ionic ratios with respect to Cl⁻ is normally used to assess the atmospheric contribution of dissolved ions in water (Singh et al., 2005). The average Na^+/Cl^- and K^+/Cl^- for marine sources are 0.85 mg/L and 0.0176 mg/L respectively. The average Na^+/Cl^- is 0.98 ± 0.09 mg/L and K^+/Cl^- is 0.51 ± 0.03 mg/L. This suggests low contributions from atmospheric and marine sources and indicates high level of contributions from rock weathering (Singh et al., 2005). The plot of the data on the Gibb's diagram showing total dissolved solids (TDS) as a function of $\text{Na}^+ / (\text{Na}^+ + \text{Ca}^{2+})$ and $\text{Cl}^- / (\text{Cl}^- + \text{HCO}_3^-)$, also support the dominance of rock weathering for surface water and groundwater and evaporation process for contaminated water samples as shown in Figure. 5(ii) and Figure. 5(iii) (Gibbs, 1970).

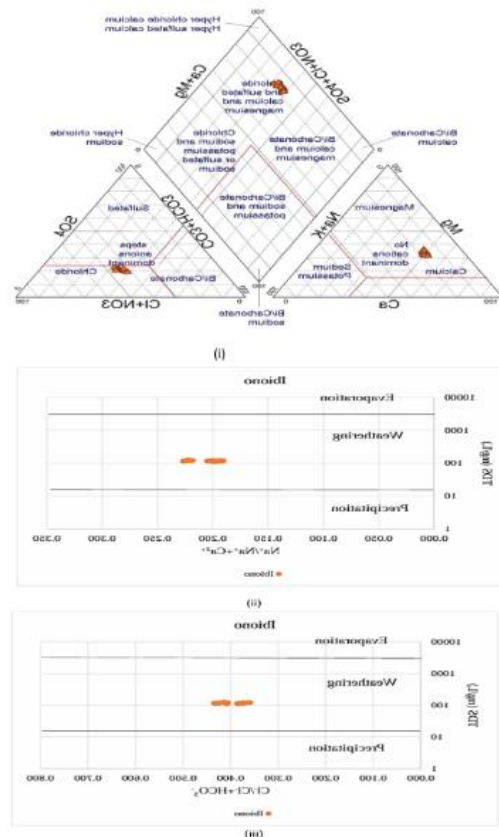


Figure 5: (i); Piper diagram plot for groundwater from the study area. (ii); Gibbs diagram for the groundwater TDS vs $\text{Na}^+ / (\text{Na}^+ + \text{Ca}^{2+})$ and (iii) TDS vs $\text{Cl}^- / (\text{Cl}^- + \text{HCO}_3^-)$

4.3.2 Ion exchange

Computed values of indices from equations based on chloroalkaline indices (CAI), Schoeller (1977):

$$CAI-1 = \left[Cl^- - (Na^+ + K^+) \right] / Cl^- \quad (13)$$

$$CAI-2 = \left[Cl^- (Na^+ + K^+) \right] / (SO_4^{2-} + HCO_3^- + NO_3^-) \quad (14)$$

Groundwater samples in this study showed prevalence for ion exchange.

4.4 Multivariate statistical analysis

4.4.1 Pearson moment correlation analysis

The interrelationships among different water quality parameters for the different water types of the study area were studied by means of Pearson moment correlation analysis. Correlation coefficients ≥ 0.70 were regarded as significant correlation. Positive correlation is noted between Na^+ and Fe and Cl^- and SO_4^{2-} indicating that the process enriching this

element might be the same (Ciner et al., 2020). Negative correlation is recorded between TDS and pH indicating that this is due to different sources of element.

4.4.2 Factor analysis

To further investigate the potential sources of the elements in the different water types, factor analysis (FA) was used to identify the most significant loadings. The results of factor analysis (FA) are presented in Table 4. Five factors with Eigen value > 1 were extracted from R-mode FA. The FA of the water quality indicated that the chemistry of the different water types in the study area is controlled by geogenic processes and anthropogenic activities. Considering the loadings in this study, factor loadings > 0.70 were considered significant and loadings < 0.70 were considered insignificant. Factor 1 explains 24.23%. This factor has significant positive (K^+) and negative (Fe) loadings for. Factor 2 explains approximately 19.93%. The factor is loaded with Cl^- and SO_4^{2-} , which is linked to anthropogenic sources. Factor 3 explains 14.01. This factor (3) is positively (TDS) and negatively (pH) loaded. Factor 4 explains 12.53% of variance. The factor is loaded with Mg^{2+} . Factor 5 which account for the variance of 10.48% is negatively (EC) and positively (HCO_3^-) loaded is suggestive of silicate and carbonate weathering.

Table 4: Factor Loadings for groundwater in the study area

LGA	Ibiono Ibom				
	Factor				
	1	2	3	4	5
Temp	0.659	-0.161	-0.175	-0.433	0.142
EC	0.072	0.322	0.048	0.061	-0.936
TDS	-0.144	-0.264	0.823	0.054	0.157
pH	0.180	-0.040	-0.899	0.080	0.053
TH	-0.358	-0.491	0.381	-0.005	0.343
Na^+	-0.640	0.571	0.352	-0.095	0.182
K^+	0.788	0.198	-0.099	0.191	0.156
Ca^{2+}	-0.282	-0.090	-0.602	0.265	0.584
Mg^{2+}	0.374	0.022	-0.087	0.792	0.140
Cl^-	0.087	0.903	0.114	0.145	-0.131
HCO_3^-	0.184	0.174	0.262	0.039	0.752
SO_4^{2-}	-0.118	0.904	-0.220	-0.145	-0.135
NO_3^-	-0.309	0.436	0.578	0.562	0.147
Fe	-0.717	0.075	0.076	-0.220	0.420
Mn	-0.001	0.279	0.136	-0.680	0.405
Eigenvalue	3.634	2.990	2.101	1.879	1.572
% Total variance	24.229	19.931	14.007	12.529	10.477
Cumulative eigen value	3.634	6.624	8.725	10.604	12.176
Cumulative %	24.229	44.160	58.167	70.696	81.172

5. CONCLUSIONS

Groundwater in the study area is largely suitable for drinking and irrigation, though localized contamination from nitrate and iron necessitates targeted intervention. The study confirms the presence of significant groundwater reservoirs in the study areas, with moderate to high groundwater potential. However, localized contamination necessitates targeted intervention strategies.

5.1 Key recommendations

Conducting aquifer vulnerability assessments and collecting additional data on aquifer parameters will enhance understanding of the hydraulic dynamics groundwater in the study area. The establishment of groundwater protection zones is recommended to prevent contamination, along with regular water quality monitoring to detect trends in hydrochemical variations. Implementing proper well-spacing strategies can help prevent over-abstraction of groundwater resources. Public awareness campaigns on safe agricultural practices and improved sanitation are also essential to protect groundwater quality in northern Akwa Ibom state. Additionally, further isotopic analyses are suggested to trace contamination sources and refine hydrogeochemical models. The integration of geophysical, hydrogeological, and hydrogeochemical data provides a robust framework for the sustainable management of

groundwater resources in the region.

REFERENCES

- Abam, T. K. S. and Nwankwoala, H. O., 2020 Hydrogeology of Eastern Niger Delta: A Review. *Journal of Water Resource and Protection*, 12, Pp. 741-777. <https://doi.org/10.4236/jwarp.2020.129045>
- Aghazadeh, N. and Mogaddam, A.A., 2010a. Assessment of groundwater quality and its suitability for drinking and agricultural uses in the Oshnavieharea, Northwest of Iran. *Journal of Environmental Protection* 1:30-40 Vol. 1 No. 1, 2010, pp. 30-40. doi: 10.4236/jep.2010.11005.
- Ajayi, O. and Umoh, O.A., 1998. Quality of groundwater in coastal plain sands aquifer of Akwa Ibom State. *Nigeria Journal of African Earth Sciences*, 27 (2): Pp. 259-275.
- American Public Health Association, (APHA), 2017. Standard methods for the examination of water and wastewater. American Public Health Association.
- Appelo, C.A.J., and Postma, D., 2005. *Geochemistry, groundwater, and pollution* (2nd ed.). CRC Press.
- Asfahani, J., 2023. Hydraulic parameters estimation by using an approach

- based on vertical electrical sounding (VES) in the semi-arid Khanasser valley region, Syria. *Journal of African Earth Science* 117: Pp. 196 – 206.
- Ayers, R.S. and Westcot, D.W., 1994. *Water Quality for Agriculture*. FAO Irrigation and Drainage Paper 29, Revision 1, FAO, Rome, 174 p.
- Back, W. and Hanshaw, B.B., 1965. *Chemical geohydrology*. Advanced Hydro Science 1. Pp. 49-109.
- Bhattacharya, P.K. and Patra, H.P., 1968. Direct current geoelectric sounding. Elsevier, Amsterdam pp 4-7.
- Bouderbala, B., Remini, A., Hamoudi, S., and Pulido-Bosch, A., 2016. Assessment of groundwater vulnerability and quality in coastal aquifers: A case study from Tipaza, North Algeria. *Arabian Journal of Geosciences* 9(3).
- Çiner, F., Sunkari, E.D., and Şenbaş, B.A., 2020. Geochemical and Multivariate Statistical Evaluation of Trace Elements in Groundwater of Niğde Municipality, South-Central Turkey: Implications for Arsenic Contamination and Human Health Risks Assessment. *Archives of Environmental Contamination and Toxicology* <https://doi.org/10.1007/s00244-020-00759-2>.
- Edet, A.E. and Okereke, C.S., 2022. Investigation of hydrogeological conditions of a fractured Shale aquifer in Yala Area (SE Nigeria) characterized by saline groundwater. *Applied Water Science* 12:194 <https://doi.org/10.1007/s13201-022-01715-2>.
- Edet, A.E., and Ntekim, E.E.U., 1996. Heavy metal distribution in groundwater from Akwa Ibom State, eastern Niger delta-A preliminary pollution assessment *Global Journal of Pure and Applied Sciences* Vol. 2 (1): Pp. 67-77.
- Edet, A.E., and Okereke, C.S., 1997. Assessment of hydrogeological conditions in basement aquifers of Precambrian Oban massif, southeastern Nigeria. *Journal of Applied Geophysics*, 36, Pp. 195–204.
- Edet, A.E., and Okereke, C.S., 2001. A regional study of saltwater intrusion in southeastern Nigeria based on analysis of geoelectrical and hydrochemical data. *Environmental Geology* 40 (10): Pp. 1278-1289.
- Edet, A.E., and Okereke, C.S., 2014. An integrated approach for aquifer characterization and evaluation in a complex geologic terrain (Cross River State, Nigeria): A contribution to support sustainable development and management of groundwater. *Journal of African Earth Sciences*, Volume 201, 2023,104894, ISSN 1464-343X, <https://doi.org/10.1016/j.jafrearsci.2023.104894>.
- Edet, A.E., 1993. Groundwater quality assessment in parts of eastern Niger Delta. *Environmental Geology*, 22, Pp. 41–46.
- Edet, A.E., 2018. Seasonal and spatio-temporal patterns, evolution and quality of groundwater in Cross River State, Nigeria: implications for groundwater management. *Sustainable Water Resources management* DOI 10.1007/s40899-018-0236-6.
- Edet, A.E., 2021. Aquifer Characteristics and Evidence of Saltwater Intrusion in Coastal Groundwater of Niger Delta (Nigeria) Based on Historical and Recent Data. In: Al-Maktoumi A. et al. (eds) *Water Resources in Arid Lands: Management and Sustain ability*. *Advances in Science, Technology and Innovation (IEREK Interdisciplinary Series for Sustainable Development)*. Springer, Cham. https://doi.org/10.1007/978-3-030-67028-3_29:345-366.
- Ekanem, A.M., George, N.J., Thomas, J.E., Udo, I.G., 2024. Geophysical investigation of aquifer flow unit characteristics in northern parts of Akwa Ibom State, Southern Nigeria, *Results in Earth Sciences*, Volume 2, 2024, 100017, ISSN 2211-7148, <https://doi.org/10.1016/j.rines.2024.100017>.
- Ekpo, I.E., Essien, U.B., and Udoh, E.S., 2018. Hydrogeophysical investigation of groundwater potential in parts of Akwa Ibom State using Vertical Electrical Sounding. *Journal of Applied Geophysics*, 76(3), Pp. 245-256.
- Esu, E.O., Okereke, C.S., and Edet, A.E., 1999. A regional hydrostratigraphic study of Akwa Ibom State, southeastern Nigeria. *Global Journal of Pure and Applied Sciences* 5 (1): Pp. 89-96.
- Federal Ministry of Water Resources (FMWR), 2021. *Water Sanitation and Hygiene national outcome routine mapping*. National Bureau of Statistics. 2021
- Fetter, C.W., 2018. *Applied hydrogeology* (4th ed.). Prentice Hall.
- Freeze, R. A. and Cherry, J. A., 2010. *Groundwater* (2nd ed.). Prentice Hall.
- George N.J., Emah J.B, and Ekong, U.N., 2015a. Geohydrodynamic properties of hydrogeological units in parts of Niger Delta, Southern Nigeria. *Journal of African Earth Sciences* 105: Pp. 55-63
- George N.J., Ibuot, J.C., and Obiora, D.N., 2015b. Geoelectrc hydraulic parameters of shallow sandy aquifer in Itu, Akwa Ibom State (Nigeria) using geoelectric and hydrogeological measurements. *Journal of African Earth Sciences* 110: Pp. 52-63.
- George, N.J., Ibanga, J.M., and Ubom, A.I., 2015c. Geoelectro hydrogeological indices of evidence of ingress of saline water into freshwater in parts of coastal aquifers of Ikot Abasi, southern Nigeria. *Journal of African Earth Sciences* 109: Pp. 37-46.
- Gibbs, R.J., 1970. Mechanisms controlling world water chemistry. *Science* 170:1088–1090.
- Iloje, N.P., 2001. *A new geography of Nigeria*. New Revised Edition. Longman, Nigeria.
- Kalaivani, K., and Krishnaveni, M., 2015. Multivariate statistical analysis of pollutants in Ennore creek, southeast coast of India. *Global NEST Journal*. *Global NEST Journal*, Vol 17, No 3, pp 618-627.
- Lkr, A., Singh, M.R., and Puro, N., 2020. Assessment of water quality status of Doyang River, Nagaland, India, using Water Quality Index. *Applied Water Science* 10, 46. <https://doi.org/10.1007/s13201-019-1133-3>.
- Maillet, R., 1947. The fundamental equations of electrical prospecting. *Geophysics*, Vol. 12, No. 4, 1947, pp. 529-556. doi:10.1190/1.1437342.
- Massoud, M., El Osta, M., Alqarawy, A., Elsayed, S., and Gad, M., 2022. Evaluation of groundwater quality for agricultural under different conditions using water quality indices, partial least squares regression models, and GIS approaches. *Applied Water Science* 12, 244. <https://doi.org/10.1007/s13201-022-01770-9>.
- Mbonu, P.D.C., Ebeniro, J.O., Ofoegbu, C.O., and Ekine, A.S., 1991. Geoelectric sounding for the determination of aquifer characteristics in parts of the Umuahia area of Nigeria. *Geophysics* 5 (2): Pp. 284–291 <https://doi.org/10.1190/1.1443042>.
- Mukherjee, I. and Singh, U.K., 2021. Characterization of groundwater nitrate exposure using Monte Carlo and Sobol sensitivity approaches in the diverse aquifer systems of an agricultural semiarid region of Lower Ganga Basin, India, *Science of The Total Environment*, Volume 787, <https://doi.org/10.1016/j.scitotenv.2021.147657>.
- Mukherjee, I. and Singh, U.K., 2022. Environmental fate and health exposures of the geogenic and anthropogenic contaminants in potable groundwater of Lower Ganga Basin, India, *Geoscience Frontiers*, Volume 13, Issue 3, <https://doi.org/10.1016/j.gsf.2022.101365>.
- Murat, R.C., 1972. Stratigraphy and paleogeography of the Cretaceous and Lower Tertiary in southern Nigeria. In Dessauvagie, T. F. G. and Whiteman, A. J. (Eds.), *African Geology*. Geology Dept., University of Ibadan, Pp. 251 – 266.
- Niwas, S. and Singhal, D.C., 1981. Estimation of aquifer transmissivity from Dar-Zarrouk Parameters in porous media, *Journal of Hydrology*, vol.50, pp.393-399,
- Onuoha, K.M. and Mbazi, F.C.C., 1988. Aquifer transmissivity from electrical sounding data: the case of Ajali sandstone aquifers, southeast of Enugu, Nigeria. In: Ofoegbu CO (ed) *Groundwater and Mineral Resources of Nigeria*. Vieweg, Braunschweig, Germany, pp 17-29.
- Piper, A.M., 1944. A graphic procedure in the geochemical interpretation of water-analyses. *EOS Transactions American Geophysical Union* 25 (6), Pp. 914–928. <http://dx.doi.org/10.1029/TR025i006p00914>.
- Schoeller, H., 1977. *Geochemistry of groundwater in Groundwater studies* (Vol. 15, pp. 1-18). UNESCO.
- Short, K.C. and Stauble, A.J., 1967. Outline of the geology of Niger Delta. *American Association of Petroleum Geologist Bulletin* 51: Pp. 661-779.

- Singh, A.K., Mondal, G.C., Singh, P.K., Singh, K., Singh, T.B., and Tewary, B.K., 2005. Hydrochemistry of reservoirs of Damodar River basin, India. *Environmental Geology* 48: Pp. 1014-1028.
- Stumm, W. and Morgan, J.J., 2012. *Aquatic chemistry: chemical equilibria and rates in natural waters*, vol 126. Wiley, New York.
- Subba Rao, N., Subrahmanyam, A., Ravi Kumar, S., Srinivasulu, N., Babu Rao, G., Surya Rao, P., and Venkatram Reddy, G., 2012. Geochemistry and quality of groundwater of Gummanampadu Sub-basin, Guntur District, Andhra Pradesh, India. *Environmental Earth Sciences* 67(5) DOI: 10.1007/s12665-012-1590-6.
- Thakre, G., Shrivastava, N., Mishra, D.D., and Bijpai, A., 2010. Limnological studies to assess the water quality of Tapti Pond at Multai District, Betul (MP). *Int J Che Sci* 8(4): Pp. 2105–2114.
- Tizro, A.T., Voudouris, K.S., Salehzade, M., and Mashayekhi, H., 2010. Hydrogeological framework and estimation of aquifer hydraulic parameters using geoelectrical data: a case study from West Iran. *Hydrogeology Journal* 18: Pp. 917-929.
- Todd, D.K., and Mays, L.W., 2005. *Groundwater hydrology* (3rd ed.). John Wiley and Sons.
- Udo, A.A., Ijeh, I.B., Eyenaka, F.D., and Agabi, D.A., 2019. Geoelectric investigation of groundwater potentials in Ini Local Government Area of Akwa Ibom State, Nigeria. *Journal of Research and Innovations in Engineering*. 4 (1), Pp. 59-70.
- Udom, G.J., 2004. *Regional Hydrogeology of Akwa Ibom State, Nigeria Using Lithological, Pump Testing and Resistivity Data*. Unpolished PhD Thesis, University of Calabar. pp 163-165.
- Udosen, N., Ekanem, A.M., George, N.J., 2024. Modeling of aquifer geo-hydraulic characteristics with geo-electrical methods at a major coastal aquifer system in Uyo, southern Nigeria. *Water Practice and Technology* 19(1) DOI: 10.2166/wpt.2024.018
- Uduak, C.U. and Ini, D.E., 2012. Analysis of Rainfall Trends in Akwa Ibom State, Nigeria. *Journal of Environment and Earth Science*, 2, 60-70.
- William, B., Onsmann, A., and Brown, T. (2010). Exploratory factor analysis: A five-step guide for novices. *Journal of Emergency Primary Health Care*, 8(3).
- World Health Organization, (WHO), 2011. *International standards for drinking water and guidelines for water quality*. Geneva: WHO.
- Zohdy, A.A.R., Eaton, G.P., and Mabey, D.R., 1974. *Application of surface geophysics to groundwater investigations*. United State Geophysical Survey, Washington.

